

Article

Not peer-reviewed version

The Possibility to Estimate In Situ the Porosity of Permafrost: A Preliminary Study

[Lev Eppelbaum](#) *

Posted Date: 22 August 2023

doi: 10.20944/preprints202308.1543.v1

Keywords: permafrost; porosity; refreezing time; shut-in temperature



Preprints.org is a free multidiscipline platform providing preprint service that is dedicated to making early versions of research outputs permanently available and citable. Preprints posted at Preprints.org appear in Web of Science, Crossref, Google Scholar, Scilit, Europe PMC.

Copyright: This is an open access article distributed under the Creative Commons Attribution License which permits unrestricted use, distribution, and reproduction in any medium, provided the original work is properly cited.

Disclaimer/Publisher's Note: The statements, opinions, and data contained in all publications are solely those of the individual author(s) and contributor(s) and not of MDPI and/or the editor(s). MDPI and/or the editor(s) disclaim responsibility for any injury to people or property resulting from any ideas, methods, instructions, or products referred to in the content.

Article

The Possibility to Estimate In Situ the Porosity of Permafrost: A Preliminary Study

L.V. Eppelbaum ^{1,2}

¹ Dept. of Geophysics, Faculty of Exact Sciences, Tel Aviv University, Ramat Aviv 6997801, Tel Aviv, Israel; levap@tauex.tau.ac.il

² Azerbaijan State Oil and Industry University, 20 Azadlig Ave., Baku AZ1010, Azerbaijan

Abstract: Knowledge of permafrost's ice and unfrozen water content is critical for predicting the permafrost behavior during ice–water–ice transition. This is especially relevant when ice and permafrost are melting in many regions under the influence of global warming. It is well-known that only a part of the formation's pore water turns into ice at 0 °C. After the further lowering the temperature, the water phase transition continues, but at gradually decreasing rates. Thus, the porous space is filled with ice and unfrozen water. The laboratory data show that frozen formations' mechanical, thermal, and rheological properties strongly depend on the moisture content. Hence, porosity and temperature are essential parameters of permafrost. In this paper, it is shown how, and by combining research in three fields: (1) geophysical exploration, (2) numerical modeling, and (3) temperature logging, it is possible to estimate *in-situ* the porosity of permafrost. To demonstrate the procedure, five examples of numerical modeling (where all input parameters are specified) are given. This investigation is the first attempt to analyze the permafrost's porosity in situ quantitatively.

Keywords: permafrost; porosity; refreezing time; shut-in temperature

1. Introduction

It is well-known that only a part of the formation's pore water turns into ice at 0 °C. With the additional lowering of the temperature, the phase transition of the water continues, however, at gradually decreasing rates. The quantity of unfrozen water is practically independent of the total moisture content for soil with the concrete physical-chemical parameters (Tsytovich, 1975). Frozen soil is the matter in which stresses and strains arise under the influence of an external load. These forces are not constant but vary with time. It gives rise to the relaxation of stresses and creeps (i.e., increased strains over time). These complex physical-chemical processes are called rheological ones. The vigorous development of the rheological processes in frozen soils is caused by the peculiarities of their internal relationships in which ice plays a significant role. Numerous laboratory experiments show that frozen formations' mechanical, thermal, and rheological properties strongly depend on the moisture content. Hence, porosity and temperature are essential parameters of permafrost. It is known that the electric resistivities of frozen sediments are affected by the freezing-thawing transition to a greater extent than the seismic velocities. In the same interval of temperatures, seismic velocities may increase by 2 to 10 times in transition to a frozen condition, whereas the electrical resistivity may increase by 3·10 – 3·102 times (Hnatiuk and Randall, 1977; Dobinski, 2011; Eppelbaum, 2021). The position of the interface of the thawing-freezing transition can be determined with the application of the surface electric resistivity method and sonic logs in wells. For instance, the transition from higher resistivity and velocity values to lower ones can be considered the thawing radius's position. Thus, the position of the radius of thawing (because of well drilling or production) can be estimated by using different geophysical exploration methods. A method of estimating the refreezing time surrounding the wellbore thawed (during drilling) formations was suggested by Kutasov and Eppelbaum (2017, 2018). Only three temperature logs taken after the freezeback are completed and are needed to apply this method. The conducted numerical modeling indicates that the dimensionless time of refreezing can be expressed as a function of two dimensionless parameters:

radius of thawing and latent heat density (Kutasov, 2006; Eppelbaum and Kutasov, 2018). From the last parameter, the porosity of formations can be estimated.

The only objective of this study is to offer a possible way to estimate permafrost's porosity in situ. This study is the first effort to determine this parameter in natural conditions. This parameter in situ estimation is of special importance when the permafrost parameters are constantly changing under the influence of global warming. To demonstrate the possibility of the new approach applicability of this new method, five cases of numerical modeling are presented.

2. Time of freezeback

Since deep wells drilling in permafrost areas usually use warm mud, a certain unknown degree of the formation thawing around the wells exists. The warm mud disturbs the borehole's temperature field, and as a result, the permafrost thaws. To calculate the static formation temperature and permafrost thickness, before conducting temperature logs, engineers must wait for some period after the entire completion of drilling. The duration of the refreezing of the layer thawed during drilling dramatically depends on the natural temperature of geological formation(s). Therefore, the rocks at the bottom of the permafrost zone freeze very slowly. A lengthy restoration period (up to ten years or more) is required to calculate the permafrost's temperature and thickness with the necessary accuracy.

As it was mentioned above, only a part of the formation's pore water changes to ice at 0°C. The phase transition temperature interval exists from numerous laboratory and field experiments. With the subsequent lowering of the temperature, the water phase transition continues (Figure 1). The temperature interval of phase transition mainly depends on the mineralogical composition of the geological formations. Let us assume that the water-ice phase transition is completed at the time t_{ep} , and at least three temperature logs were taken after refreezing of thawed formations (Figure 1).

Kutasov and Eppelbaum (2003, 2017, 2018) have shown that the cooling process at $t > t_{ep}$ (Figure 1) is like that of temperature recovery in borehole sections below the permafrost base (i.e., unfrozen formations). Let us assume that thermal recovery's starting point is $t = t_{ep}$. Thus, the thermal disturbance time is $td + t_{ep}$, where td is the time of drilling mud circulation at a given depth. It will be explained below that the subsequent borehole cooling can be approximated by a constant linear heat source (per unit of length) after refreezing.

Hence, a modified Horner equation (in some publications, this method is called KEM (for instance, Bassam et al., 2010; Liu et al., 2016)) can be used to predict frozen formations' temperature to estimate the formation temperature (Kutasov and Eppelbaum, 2017, 2018). Then

$$T_s(t_s, r_w) = B \ln \left(1 + \frac{t_d + t_{ep}}{t_s - t_{ep}} \right) + T_f, \quad B = \frac{q}{4\pi\lambda}, \quad (1)$$

Then the values of shut-in temperatures can be determined (Figure 1):

$$T_{s1} = B \ln \left(1 + \frac{t_d + t_{ep}}{t_{s1} - t_{ep}} \right) + T_f, \quad (2)$$

$$T_{s2} = B \ln \left(1 + \frac{t_d + t_{ep}}{t_{s2} - t_{ep}} \right) + T_f, \quad (3)$$

$$T_{s3} = B \ln \left(1 + \frac{t_d + t_{ep}}{t_{s3} - t_{ep}} \right) + T_f. \quad (4)$$

Combining Eqs. (2) – (4), Eq. (5) is obtained for estimating the time of refreezing (t_{ep}).

$$\frac{T_{s1} - T_{s2}}{T_{s1} - T_{s3}} = \frac{\ln \left(1 + \frac{t_d + t_{ep}}{t_{s1} - t_{ep}} \right) - \ln \left(1 + \frac{t_d + t_{ep}}{t_{s2} - t_{ep}} \right)}{\ln \left(1 + \frac{t_d + t_{ep}}{t_{s1} - t_{ep}} \right) - \ln \left(1 + \frac{t_d + t_{ep}}{t_{s3} - t_{ep}} \right)}. \quad (5)$$

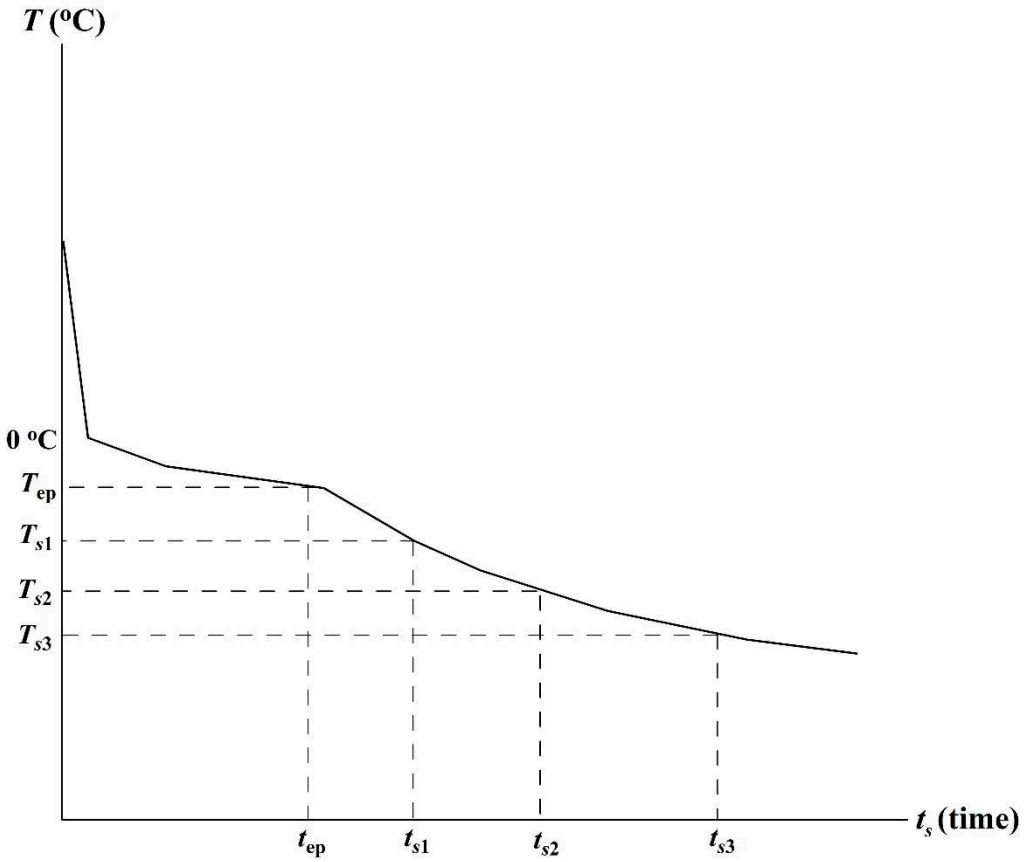


Figure 1. Shut-in temperatures at a given depth – schematic curve.

For solving Eq. (5), Newton's method was used (Grossman, 1977). In this method, a solution to an equation is obtained by defining a sequence of numbers that become successively nearer and nearer to the expected solution (Kutasov and Eppelbaum, 2017, 2018).

The parameter B is found from the following equation:

$$T_{s1} - T_{s2} = B \left\{ \ln \left(1 + \frac{t_d + t_{ep}}{t_{s1} - t_{ep}} \right) - \ln \left(1 + \frac{t_d + t_{ep}}{t_{s2} - t_{ep}} \right) \right\}. \quad (6)$$

Furthermore, the temperature of formations can be obtained from Eqs. (2) – (4).

3. The empirical formula

It was assumed that the heat flow influence from the thawed zone to the thawed zone – frozen zone interface could be neglected. The results of hydrodynamical modeling have established that this is an acceptable assumption (Eppelbaum et al., 2014). In this case, the Stefan equation – energy conservation condition at the phase change interface ($r = h$) can be applied

$$\lambda_f \frac{dT_f(r,t)}{dr} |_{r=h} = Lw \frac{dh}{dt}. \quad (7)$$

Assuming the semi-steady temperature distribution in the frozen zone (a conventional assumption):

$$T_f(r,t) = T_f \frac{\ln r/h}{\ln r_{if}/h}, \quad (8)$$

where r_{if} is the radius of thermal influence during the freezeback period. The ratio $D_f = r_{if}/h$ was obtained from a numerical solution. A computer program (Kutasov, 1999) was used to find a

numerical solution for a system of differential heat conductivity equations for frozen and thawed zones and the Stefan equation. It was found that

$$D_f = 2.00 + 0.25 \ln(I_f + 1), \quad (9)$$

$$1.5 < I_f \leq 400, \quad 1.25 < H < 23.4 \quad H = h/r_o,$$

$$I_f = -\frac{L\varphi\rho_w a_f}{T_f \lambda_f} = -\frac{L\varphi\rho_w a_f}{T_f \rho a_f c_f} = -\frac{L\varphi\rho_w}{T_f \rho_f c_f}, \quad \lambda_f = a_f \rho_f c_f, \quad (10)$$

where I_f is the dimensionless latent heat density, L is the latent heat per unit of mass, c_f is the specific heat of the formation, φ is the porosity, ρ_w is the water density, ρ_f is the formation density, r_o is the well radius, h is the radius of thawing, λ_f and a_f are the thermal conductivity and diffusivity of the frozen formations, respectively.

From Eqs. (7) – (9) and the condition $H(t_{ep}) = 1$, it was obtained (Kutasov, 2006)

$$t_{epD} = \frac{a_f t_{ep}}{r_w^2} = \frac{D_f I_f}{2} (H^2 - 1), \quad (11)$$

where t_{epD} is the dimensionless time of refreezing.

4. Numerical modeling: five cases

Taylor (1978) introduced a cylindrically symmetric source of thermal disturbance in a semi-infinite medium for the analysis of thermal borehole measurements. A numerical model has been developed to simulate the rising transient thermal regime in the mentioned model. The assumed medium is a permafrost sandstone formation. The model allows for a change of phase (ice-water, water-ice). In this model, only heat transfer by radial conduction is considered. The following parameters are introduced: the radius of cylindrical source $r_o = 0.17\text{m}$, the radial variable r , the thermal conductivity of frozen formation $\lambda_f = 4.40\text{--}3.84 \text{ W m}^{-1}\text{K}^{-1}$, the thermal conductivity of unfrozen formation $\lambda_{un} = 3.84 \text{ W m}^{-1}\text{K}^{-1}$, specific heat $c_f = 950$, $c_{un} = 1138 \text{ J kg}^{-1}\text{K}^{-1}$, the density of sandstone $\rho_f = 2483 \text{ kg m}^{-3}$, the density of water/ice $\rho_w = 1000 \text{ kg m}^{-3}$, the porosity $\varphi = 0.09$, the density of water/ice $\rho_w = 1000 \text{ kg m}^{-3}$, and latent heat $L = 334960 \text{ J kg}^{-1}$ for the water/ice boundary. The latent heat density of the medium is $\chi = L\rho_w\varphi = 334960 \cdot 1000 \cdot 0.09 = 30 \cdot 10^6 \text{ J m}^{-3}$. The duration of source disturbance is t_d . The temperature of 0°C is assumed as a phase change. The calculated data in Tables 1–4 are given for initial temperatures (T_f): -0.01° , -5° , -10° C for source temperatures (T_w): 10°C and 30°C . In the construction of Tables 1–4, dimensionless distance and dimensionless time were used:

$$R = \frac{r}{r_o}, \quad t_{dD} = \frac{a_f t_d}{r_o^2}, \quad t_{sD} = \frac{a_f t_s}{r_o^2}, \quad a_f = \frac{\lambda_f}{c_f \rho_f},$$

$$t_s = t - t_d.$$

Table 1. Input data for 2 cases of numerical modeling (Taylor, 1978, pp. 56 and 57). T_w is the temperature of the cylindrical source, T_s is the shut-in temperature, and T_f is the temperature of formation.

Case 1		Case 2	
$T_w = 10^\circ\text{C}$,		$T_w = 10^\circ\text{C}$,	
$T_f = -10^\circ\text{C}$,		$T_f = -10^\circ\text{C}$,	
$t_{dD} = 100$		$t_{dD} = 300$	
t_{sD}	$T_s, ^\circ\text{C}$	t_{sD}	$T_s, ^\circ\text{C}$

20	0.00	30	0.00
30	0.00	60	-1.19
40	-3.32	90	-4.24
50	-4.52	120	-5.29
70	-5.80	150	-5.96
100	-6.81	210	-6.80
200	-8.18	300	-7.53
300	-8.72	400	-8.02
400	-9.01	500	-8.34
500	-9.19	600	-8.57
600	-9.31	700	-8.74
700	-9.41	1700	-9.47
800	-9.48		
900	-9.53		

Table 2. Input data for three cases of numerical modeling (Taylor, 1978, pp. 73, 50, 65).

t_{sD}	$T_s, ^\circ C$	t_{sD}	$T_s, ^\circ C$	t_{sD}	$T_s, ^\circ C$
Case 3		Case 4		Case 5	
$T_w = 30^\circ C,$		$T_w = 10^\circ C,$		$T_w = 30^\circ C,$	
$T_f = -10^\circ C,$		$T_f = -5^\circ C,$		$T_f = -5^\circ C,$	
$t_{dD} = 1000$		$t_{dD} = 30$		$t_{dD} = 30$	
400	0.0	30	0.0	60	0.0
500	0.0	40	0.0	70	0.0
700	-3.52	50	-1.22	170	-2.58
800	-4.45	60	-2.32	270	-3.66
900	-5.09	70	-2.61	370	-4.05
1000	-5.58	170	-4.15	470	-4.27
2000	-7.93	270	-4.46	570	-4.40
3000	-8.91	370	-4.61	670	-4.49
4000	-9.43	470	-4.69	770	-4.56
5000	-9.70	570	-4.74	870	-4.61
				970	-4.65

Table 3. Results of calculations for cases 1 and 2. T_{fcal} is the calculated formation temperature. Input data are presented in Table 1.

1	2	3	4	5	6	7	8
t_{s1D}	t_{s2D}	t_{s3D}	t_{epD}	$B, ^\circ C$	$T_{fcal}, ^\circ C$	I_f	Φ
Case 1. $H = 3.87; T_f = -10^\circ C$							
50	70	900	18.5	3.49	-9.97	1.205	0.086
50	70	800	18.5	3.50	-9.97	1.205	0.086
50	70	700	18.5	3.49	-9.97	1.205	0.086

50	70	600	18.7	3.46	-9.95	1.217	0.087
50	70	500	18.7	3.46	-9.95	1.217	0.087
50	70	400	18.8	3.45	-9.95	1.223	0.087
50	70	300	19.1	3.43	-9.93	1.241	0.089
50	70	200	19.6	3.37	-9.89	1.272	0.091
40	70	200	21.3	3.25	-9.86	1.375	0.098
40	70	300	20.9	3.31	-9.91	1.351	0.096
40	70	400	20.7	3.34	-9.93	1.339	0.096
40	70	500	20.6	3.35	-9.94	1.333	0.095
40	70	600	20.5	3.36	-9.94	1.327	0.095
Case 2. $H = 4.80$; $T_f = -10$ °C							
90	120	210	37.5	2.78	-9.81	1.525	0.109
90	120	300	36.7	2.82	-9.85	1.494	0.107
90	120	400	35.9	2.86	-9.89	1.464	0.105
90	120	500	35.6	2.87	-9.90	1.452	0.104
90	120	600	35.4	2.89	-9.92	1.445	0.103
90	120	700	35.3	2.89	-9.92	1.441	0.103
90	120	1700	33.3	3.00	-10.02	1.364	0.097
120	210	300	32.0	2.96	-9.92	1.314	0.094
120	210	400	30.4	3.01	-9.94	1.252	0.089
120	210	500	30.3	3.02	-9.95	1.248	0.089
120	210	600	29.9	3.03	-9.95	1.233	0.088
120	210	700	30.0	3.03	-9.95	1.237	0.088

Table 4. Results of calculations for cases 3-5. T_{fcal} is the calculated formation temperature. Input data are presented in Table 2.

60	170	570	45.8	1.11	-5.01	2.704	0.096
60	270	570	46.5	1.09	-5.01	2.742	0.098
60	370	570	48.8	1.00	-4.99	2.868	0.102
Case 5. $H = 6.42$; $T_f = -5^\circ\text{C}$							
270	470	970	118.4	1.491	-4.99	2.544	0.091
270	570	970	113.7	1.550	-5.00	2.451	0.088
270	670	970	109.0	1.611	-5.00	2.356	0.084

Thus, t_d is the time of thermal disturbance, and t_s is the "shut-in" time. The radial temperature distributions during the thermal disturbance (T_d) and "shut-in" (T_s) periods are presented as follows:

$$T_d(R, t_{dD}) = f(R, t_{dD}), \quad T_s(R, t_{sD}) = f(R, t_{sD}).$$

In Tables 1 and 2, the values of $T_s = T_s(R = 1, t_{sD})$ are used.

5. Results of calculations

At this stage, to use Eqs. (1) – (6) the following parameters will be relaxed

$$t_d, \quad t_s, \quad t_{ep}, \quad t_{s1}, \quad t_{s2}, \quad t_{s3}$$

by its dimensionless values

$$t_{dD} = \frac{a_f t_d}{r_o^2}, \quad t_{sD} = \frac{a_f t_s}{r_o^2}, \quad t_{epD} = \frac{a_f t_{ep}}{r_o^2}, \quad t_{s1} = \frac{a_f t_{s1}}{r_o^2}, \quad t_{s2} = \frac{a_f t_{s2}}{r_o^2},$$

$$t_{s3} = \frac{a_f t_{s3}}{r_o^2}.$$

The results of calculations after Eqs. (1) – (6) (in the dimensionless units) are presented in Tables 3 and 4 (columns 4-6).

As can be seen from Table 3 for case 1, the calculated dimensionless refreezing time varies in the restricted limits (18.5-21.3). At the same time, the results of numerical modeling provide corresponding values of 20-30 (Table 1, values in bold). For cases 2-5, the calculated refreezing times (Tables 3 and 4, column 4) agree with the results of mathematical modeling (Tables 1 and 2, values in bold).

The dimensionless thawing radius was defined as the position of the 0°C isotherm and was found from $T_d = f(R, t_{dD})$ as $0^\circ\text{C} = f(R = H, t_{dD})$. Here linear interpolation was used.

From Eq. (11) follows that the dimensionless latent heat density (I_f) can be determined as a function of dimensionless refreezing time and thawing radius. As at the solution of implicit Eq. (6), Newton's method was again used to estimate the value of I_f from Eq. (11). The calculation results are presented in Tables 3 and 4 (column 7).

And finally, the porosity is found from Eq. (10)

$$\varphi = -\frac{I_f T_f \rho_f c_f}{L \rho_w}, \quad (12)$$

The calculation results are displayed in Tables 3 and 4 (column 8).

It also should note that for cases 1, 2, 4, and 5, the calculated values of formation temperature (Tables 3 and 4, column 6) are in excellent agreement with the assumed values ($T_f = -5^\circ\text{C}$ and -10°C) at numerical modeling. The difference $T_f - T_{fcal}$ for case 3 can be explained by the low accuracy in determining the radius of thawing. As mentioned earlier, the linear interpolation method was used

to estimate the thawing radius. Figure 2 also shows that the basic formula 1 (in dimensionless units) can be used to estimate the transient shut-in temperature.

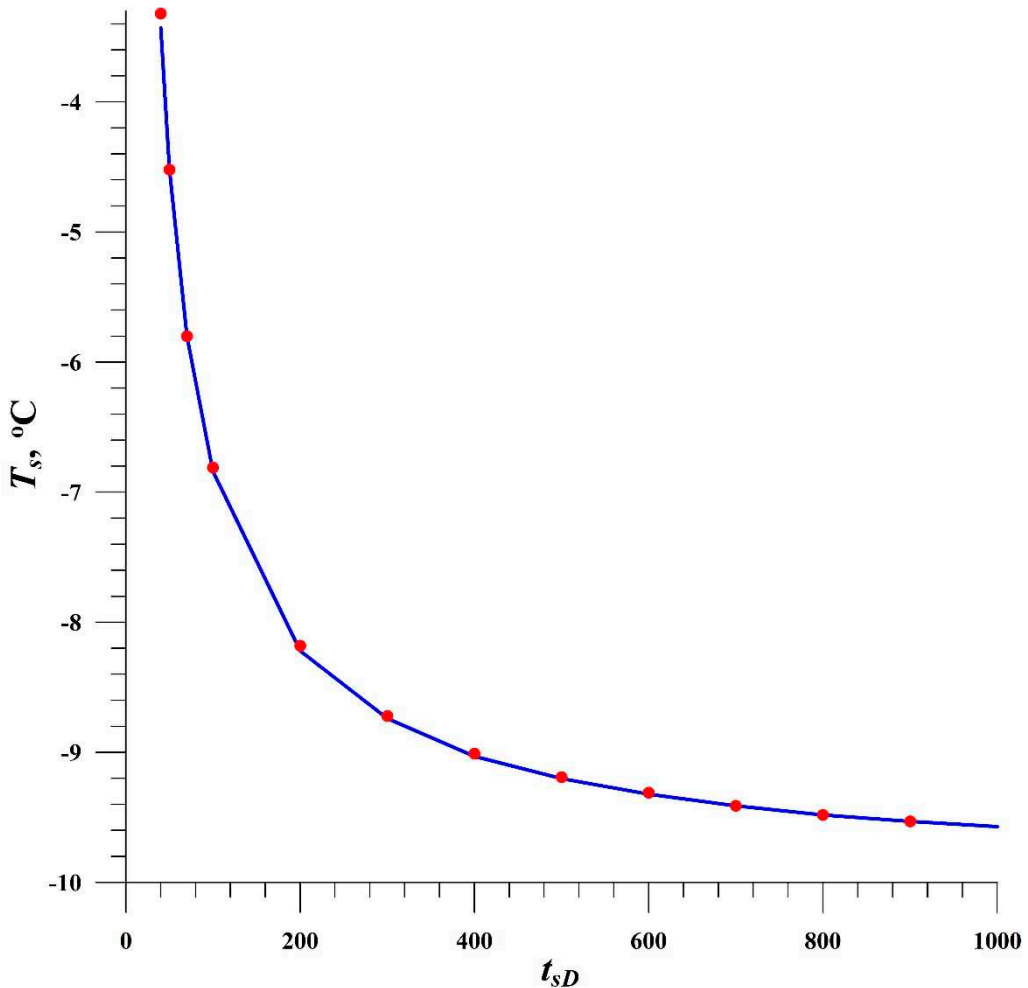


Figure 2. Transient shut-in temperature. Case 1, $B = 3.39$ °C, $T_{fcal} = -10$ °C, $t_{dD} = 100$, $t_{epD} = 18.5$. The solid line is constructed using Eq. (1); points present the results of numerical modeling.

6. Discussion and Conclusions

The estimated porosity (φ) values are presented in Tables 3 and 4 (column 8). For case 1, the φ values vary in narrow limits 0.086-0.095. The ranges for cases 2-5 are: 0.088-0.109; 0.081-0.011; 0.096-0.102; and 0.084-0.091, correspondingly. Thus, the average porosity values in all five cases are very close to the assumed numerical modeling value of $\varphi = 0.09$. The results of calculations shown in Tables 3 and 4 (columns 4-8) testify that the basic formulas 1, 5, and 11 approximate the results of the numerical modeling with the necessary accuracy.

It should note that all input parameters (dimensionless heating and “shut-in” time, latent heat density, thermal properties of the formation a.o.) were specified in numerical modeling. Only the dimensionless thawing radius was defined as the position of the 0 °C isotherm and was found from tables $T_d = f(R, t_{dD})$ as 0 °C = $f(R = H, t_{dD})$. From the implicit Eq. (11) follows that the dimensionless latent heat density is a function of two parameters: dimensionless thawing radius (H) and dimensionless refreezing time (t_{epD}). Thus, to estimate the porosity of permafrost in field conditions (*in-situ*), it is essential to determine the values H and t_{epD} by temperature logging and other geophysical methods. For this reason, this work can be considered as a preliminary study. As it was mentioned earlier, the position of the interface of the thawing-freezing transition (radius of thawing) can be verified with geophysical methods – sonic logs and electric resistivity. Kutasov and Eppelbaum (2017, 2018) presented three examples of estimation of the refreezing time using

temperature logging results. Furthermore, to validate the approach presented in this paper, the calculated porosity values should be compared with those obtained from cuttings and samples.

References

Bassam, A., Santoyo E., Andaverde, J., Hernández, J.A. and Espinoza-Ojeda, O.M., 2010. Estimation of static formation temperatures in geothermal wells by using an artificial neural network approach. *Computers & Geosciences*, **36**, No. 9, 1191-1199. <https://doi.org/10.1016/j.cageo.2010.01.006>

Dobinski, W., 2011. Permafrost. *Earth-Science Reviews*, **108**, 158-169. <https://doi.org/10.1016/j.earscirev.2011.06.007>

Eppelbaum, L.V., 2021. VLF-method of geophysical prospecting: A non-conventional system of processing and interpretation (implementation in the Caucasian ore deposits). *ANAS Transactions, Earth Sciences*, No. 2, 16-38. <https://doi.org/10.33677/ggianas20210200060>

Eppelbaum, L.V. and Kutasov, I.M., 2019. Well drilling in permafrost regions – dynamics of the thawed zone. *Polar Research*, **38**, No. 2, 1-9. <https://doi.org/10.33265/polar.v38.3351>

Eppelbaum, L.V., Kutasov, I.M. and Pilchin, A.N., 2014. *Applied Geothermics*. Springer, Heidelberg – N.Y.

Grossman, S.I., 1977. *Calculus*. Academic Press, NY - San Francisco - London.

Hnatiuk, J. and Randall, A.G., 1977. Determination of permafrost thickness in wells in Northern Canada. *Canad. Jour. Earth Sci.*, **14**, 375-383. <https://doi.org/10.1139/e77-038>

Kutasov, I.M., 1999. *Applied Geothermics for Petroleum Engineers*. Elsevier, Amsterdam.

Kutasov, I.M., 2006. Radius of thawing around an injection well and time of complete freezback. *Jour. of Geophysics and Engineering*, **3**, 154-159. <https://doi.org/10.1088/1742-2132/3/2/006>

Kutasov, I.M. and Eppelbaum, L.V., 2003. Prediction of formation temperatures in permafrost regions from temperature logs in deep wells – field cases. *Permafrost and Periglacial Processes*, **14**, No. 3, 247-258. <https://doi.org/10.1002/ppp.457>

Kutasov, I.M. and Eppelbaum, L.V., 2017. Time of refreezing of surrounding the wellbore thawed formations. *Intern. Jour. of Thermal Sci.*, **122**, 133-140. <https://doi.org/10.1016/j.ijthermalsci.2017.07.031>

Kutasov, I.M. and Eppelbaum, L.V., 2018. Corrigendum to “Time of refreezing of surrounding the wellbore thawed formations” in *Intern. Jour. of Thermal Sci.* 133–140, *Intern. Jour. of Thermal Sci.*, **124**, 548. <https://doi.org/10.1016/j.ijthermalsci.2017.10.006>

Liu C., Li K., Chen Y., Jia, L. and Ma, D., 2016. Static Formation Temperature Prediction Based on Bottom Hole Temperature. *Energies*, **9**, 646, 1-14. <https://doi.org/10.3390/en9080646>

Taylor, A.E., 1978. *Temperatures and Heat Flow in a System of Cylindrical Symmetry Including a Phase Boundary*. Geothermal Series, 7, Ottawa, Canada.

Tsytovich, N.A., 1975. *The Mechanics of Frozen Ground*. Scripta Book Co., Washington, D. C.

Disclaimer/Publisher's Note: The statements, opinions and data contained in all publications are solely those of the individual author(s) and contributor(s) and not of MDPI and/or the editor(s). MDPI and/or the editor(s) disclaim responsibility for any injury to people or property resulting from any ideas, methods, instructions or products referred to in the content.